INFLUENCE OF WELDING VARIABLES ON RESISTANCE WELDING OF DISSIMILAR METALS QUALITY.

***Khafagy, S. M.*[*,‡] *and El-Shennawy, M.*[†]

[*]*Tabbin Institute for Metallurgical Studies (TIMS), P.O. Box: 109 Helwan, Cairo, Egypt.*

[†]*Mechanical Engineering Department, Faculty of Engineering, Helwan University, Helwan, Cairo, Egypt.*

[‡]*E-mail: egtimsmmk@hotmail.com*

ABSTRACT

The investigation explains the influence of important variables of resistance joining process on the characteristics of spot welded joint between low carbon steel LCS with 0.6 mm thickness and stainless steel type 430, FSS with 0.5 mm thickness sheets. Variables investigated are electrode pressure, current, and time of welding. Mechanical and metallurgy l properties are measured through microstructure, shear tensile and hardness determination. It is shown that the effective electrode pressure in this combination of FSS and CS was 2 bar (0.2MPa). It is noted that the current of welding is the effective variable on weld properties. The highest strength of weld is achieved at 3.4 KA. Rising welding time and welding current up to certain limit raises the strength of spot welded joint, after this limit, the strength of welded joint reduces. The microstructure of nugget obtained is martensitic structure. The fracture of spot welded joint is characterized by intergranular fracture in side of ferritic stainless steel sheet and the fracture mode is button pullout. The highest values of micro hardness distribution are observed at locations where carbides precipitated beside nugget martensitic structure.

Keywords

Spot welding; dissimilar welding; weld quality; controlling parameters; ferritic stainless steel; metallurgical and mechanical characteristics.

1. INTRODUCTION

Resistance spot welding is widely used and applied in many industrial productions because of its high speed and adaptability for automation in high-rate production of sheet metal assemblies. It is also faster process than other joining processes and requires less operator skills to achieve it, which make spot welded joint economical in many job shop processes [1-3]. As needs of the products having low cost and weight, dissimilar sheet metal assemblies have being used in automotive industries [4]. It is applied for joining low carbon steel components for the bodies and chassis of automobiles, buses, trucks and office furniture [5–7].

Austenitic stainless steels and low carbon steels are joined similarly [8-9] and dissimilarly [10-11] by using resistance spot welding technique. Dissimilar welding between ferritic stainless steel and low carbon steel by using spot welding received limited attention and, therefore limited information about it is available. Ferritic stainless steel AISI 430 grade and low carbon steel were the dissimilar materials selected for this study. Effect of main welding parameters on weld quality of these steels has been studied. Those parameters included welding current, welding pressure

(electrode force) and welding time. Weld quality was evaluated based mainly on weld strength. Therefore, microstructure observation and micro hardness and tensile shear examination for the dissimilar weld were achieved to evaluate variables of resistance spot welding influence of the of FSS steel and LCS sheets weldability.

2. MATERIALS AND EXPERIMENTAL METHODS

2.1. Materials and Welding Process

The low-carbon steel having 0.6 mm thickness and ferritic stainless steel grade 430 having 0.5 mm thickness are utilized in this investigation. Chemical analysis and mechanical properties of steels combination are explained in tables 1 and 2. The materials were prepared into pieces with dimensions of 150 mm x 25 mm. combination of metal sheets were resistance spot welded applying spot welding machine of 0–17.5 KA weld current. Spots were achieved by utilizing water-cooled electrode. Welding was done as overlapping joint to fabricate the specimens for mechanical test shown as in figure 1. Table 3 gives, various welding variables were used to determine their effects on spot welded joints properties. The influence of applied pressure and welding current and time were studied in this investigation work. Figure 2 shows failure samples of the resistance spot dissimilar welded specimens as the result of tensile shear test.

2.2. Mechanical Testing and Metallographic Examination

Figure 3 shows tensile shear test, which was achieved for all spot welded specimens. The micro hardness distribution for the spot welded joint regions (HAZ and base materials' and nugget) of some selected specimens was determined.

Metallographic observation and fracture surface examination for selected specimens are achieved by using optical and scanning electron SEM microscopes.

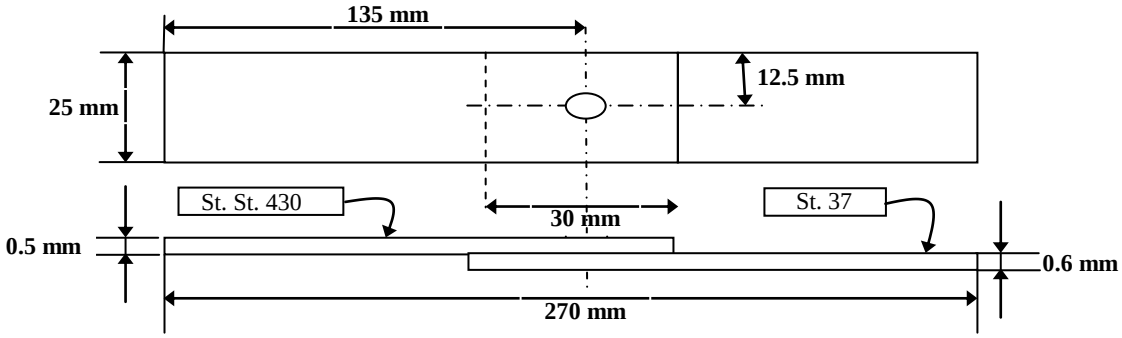

Fig. 1: Schematic of dissimilar resistance spot-welded joint.

Table (1): Chemical compositions for the sheet metals used.

Steel	C	Si	Mn	P	S	Cr	Mo	Ni
	0.06	0.29	0.22	0.03	0.002	15.6	0.05	0.21
AISI 430	**Al**	**Co**	**Cu**	**Nb**	**Ti**	**V**	**W**	**Fe**
	<0.001	0.02	0.29	0.007	0.003	0.09	0.023	83.13
Low-carbon steel	**C**	**Si**	**Mn**	**P**	**S**	**Cr**	**Mo**	**Ni**
	0.08	0.009	0.17	0.016	0.006	0.01	0.0016	0.014
	Al	**Co**	**Cu**	**Nb**	**Ti**	**V**	**W**	**Fe**
	0.112	0.007	0.004	0.0008	0.0006	0.004	0.02	99.54

Table (2): Mechanical properties for materials used.

Properties / Steel	σ_T MPa	0.2 %, σ_y MPa	Elongation %	ASTM Specification
AISI 430	450	205	22	**A 176, A 240**
Low-carbon steel	315	193	18	---

Table (3): Variables applied for the dissimilar resistance spot welded joints.

variable Parameter	constant parameters		variable Parameter	Constant parameters		variable Parameter	constant parameters	
A, amp (x1,000)	P, MPa	T, cycle	T, cycle	P, MPa	A, amp (x1,000)	P, MPa	T, cycle	A, amp (x1,000)
2.5	0.2	6 & 10	2	0.2	3 & 3.4	0.14	6, 8 & 10	3 & 3.4
2.8			3			0.16		
3.0			5			0.18		
3.2			6			0.20		
3.4			7			0.22		
3.7			8			0.24		
			10					
			11					

A: Welding current, amperage
P: Welding pressure, bar
T: Welding time, cycles

(a) Effect of current (b) Effect of time (c) Effect of pressure

Fig. 2: Fractured samples of spot-welded joint resulted from tensile shear test for different conditions.

Fig. 3: Tensile shear test for the resistance spot-welded joint.

3. RESULTS AND DISCUSSION

3.1. Influence of Welding Pressure

The heat generated Q is expressed by the Formula $Q = I^2Rt$ where in this formula R is joint resistance, t is duration of current and I is current used. The resistance R is influenced by welding pressure through its effect on resistance of contact area at the interface between the work pieces. Welding pressure is generated by the force applied by the electrodes on the joint [1]. Therefore, the welding pressure is accounted as an indirect effective variable on heat generated. The influence of welding pressure on weld strength has been studied through the using of different welding pressures and evaluation the resulted weld quality. Figure 4 shows the effect of welding pressure on weld strength at different welding time and welding current values.

From figure 4, at welding current 3.4KA and welding time 10 cycles, the fracture load rises with increasing welding pressure up to 0.2 MPa then fracture load reduces with increasing welding pressure more than that value. Increasing electrode pressure above 0.2MPa, resulted in increasing contact area and hence decreasing the contact resistance, which led to reduce the heat generated at the interface. To overcome this decrease, welding time or welding current should be raised. Welding current was raised but failure in the specimens was observed for that thicknesses and welding could not be achieved.

Effect of welding pressure on weld quality was studied at different welding time and welding current values. The linear relation was observed when welding current reduced to 3.0KA with either welding time reduced to 8 or 6 cycles. The influence of pressure could be observed when current reaches its optimum value of 3.4KA.

The pressure was kept constant at 0.2MPa for the rest of the experiments because of such result. The relationship between welding energy, applying the formula of Q, and the fracture force indicated that welding pressure of 0.2MPa obtained the best joint quality.

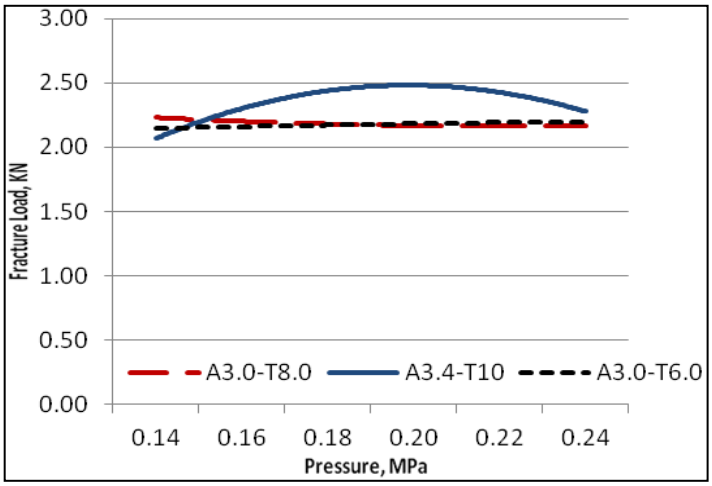

Fig. 4: Influence of welding pressure on fracture load.

3.2. Influence of Welding Current

Current is considered as an important variable in the resistance spot welding process because it has the greater effect on the heat generation than time and resistance according to formula of *Q*. With 0.2MPa pressure of welding electrode, welding current has been changed to detect its effect on fracture load. Increasing welding current from 2.5KA to 3.7KA (the maximum usable current for this condition), the fracture load increases and reaches its maximum at welding current about 3.4KA which recorded 2.78KN and then reduces to 2.57MPa as observed in figure 5. Excessive current will lead to molten metal explosion [12, 13, 17, and 18] as shown in figure 6 resulting in increasing the depth of indentation, which lower mechanical strength properties. This demonstrates the reduce strength of welded joint with current above 3.4KA.

Effect of welding current on weld strength has been investigated at lower welding time, 6 cycles. There is direct linear relation between fracture load and welding current [14]. Decreasing time reduced the heat generated that influenced the relation shown in figure 5.

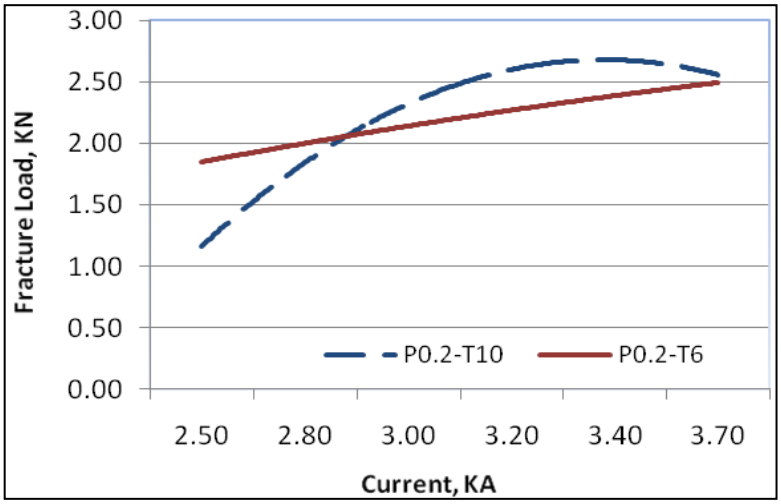

Fig. 5: Effect of welding current on fracture load.

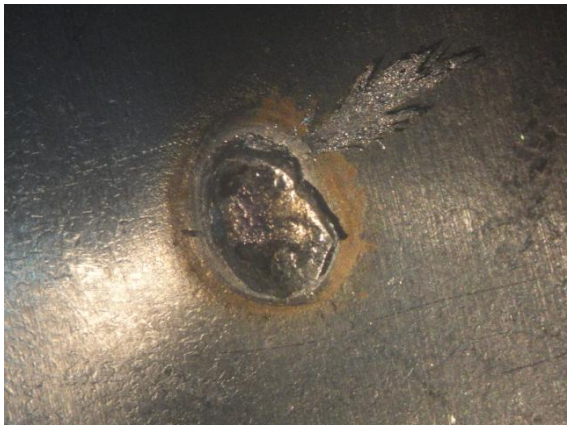

Fig. 6: Exploded molten metal from nugget.

3.3. Influence of Welding Time

Heat transferred by conduction into the surrounding base metal and electrodes and small amount transferred by radiation are considered as loses [1]. Increasing welding time raises these losses. Welding current of 3.0KA and 3.4KA has been chosen to check the effect of welding time on fracture load. As shown in figure 7 rising welding time from 2 cycles to 7 cycles raises the fracture load from 1.45 to 2.91KN and then reduces to 2.2KN with rising welding time from 7 cycles to 11 cycles. With 3.4KA, welding current, linear relationship became the prevailing phenomenon where fracture load increases with welding time rise. Two intersecting points are noticed in this relation shown in figure 7, namely at 4.5 cycles and 8.5 cycles welding time.

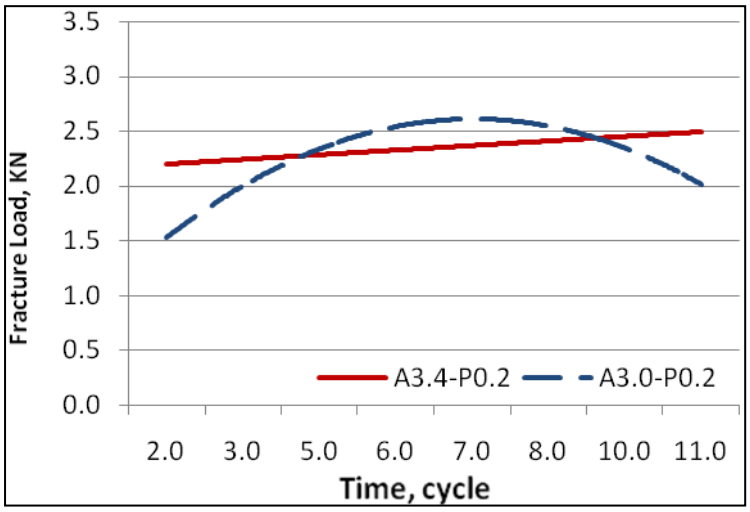

Fig. 7: Time of welding effect on fracture load.

3.4. Microstructure

The different of thermal conductivity and melting point of dissimilar metal welding affect the melting time for each side. This will result in different nugget size at each material side [19]. As clearly shown in figure 8, the nugget size of FSS side of welded material was observed bigger than that of CS. Therefore, the weld nugget lost its symmetric form. Furthermore, LCS sheet is slightly thicker thickness than that of FSS

sheet, which increased the cooling rate at LCS side leading to decreased nugget size at this side.

The HAZ microstructure of the FSS side is consisting of two regions as shown in figure 9 (a). First region, which is the adjacent to the fusion line, where subjected to high temperature, has large ferritic grains. Second region is ferritic-martensitic structure [16]. The martensitic is present surrounding the ferrite grain boundaries [7, 10] as shown in figure 9 (b). It is also found as Ẅidmanstatten side plate shape that nucleate from the grain boundary and also from intergranular as shown in figure 10. Thickness of each region is dependent on the heat input. Increasing heat energy leads to rising first region and reducing the second one. Decreasing heat generated in welding leads to eliminate the first region totally and the second one became the dominant zone at HAZ of the FSS. It is worth mentioning that the specimen shown in figure 9 (b) where its welding current and time were 3KA and 8 cycles, respectively recorded fracture load of 2.13KN. And the specimen of figure 9 (a) where its welding current and time were 3.7KA and 10 cycles, respectively recorded fracture load of 2.57KN. It is apparent that the lesser heat generated resulted in lesser fracture strength.

Fig. 8: Macrostructure of Nugget.

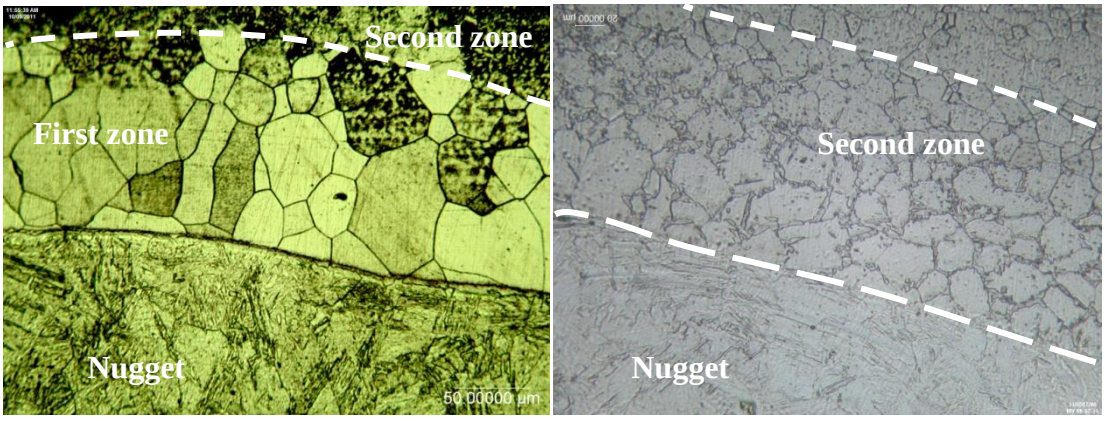

(a) I = 3.7KA, t = 10 cycles. (b) I = 3.0KA, t = 8 cycles.

Fig. 9: Weld zone and HAZs for two different spot welded joints.

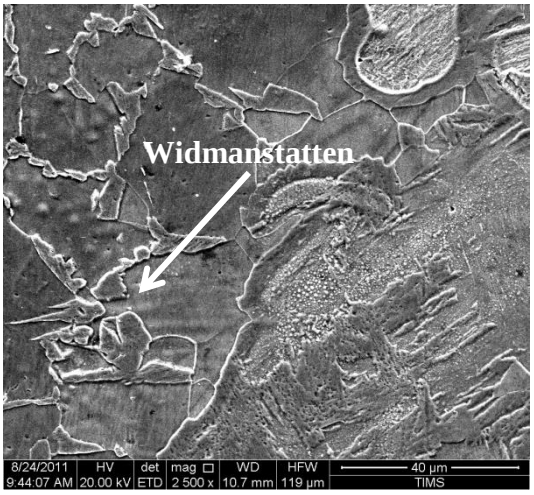

Fig. 10: More detail by SEM for specimen shown in figure 8(b).

The dominant HAZ structure at the nugget tip is ferritic structure with large grain size. This is observed for all welded specimens at different conditions as shown in figure 11.

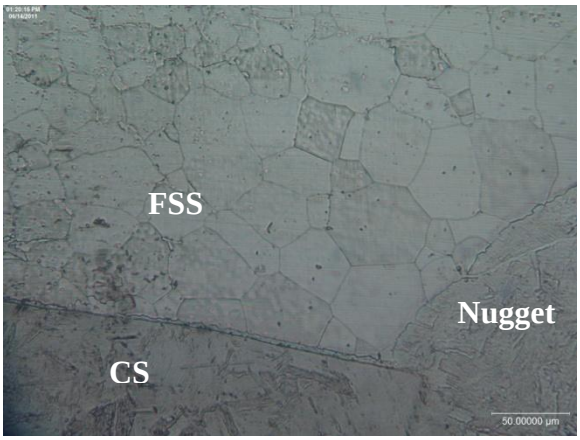

Fig. 11: HAZ microstructure at the nugget tip.

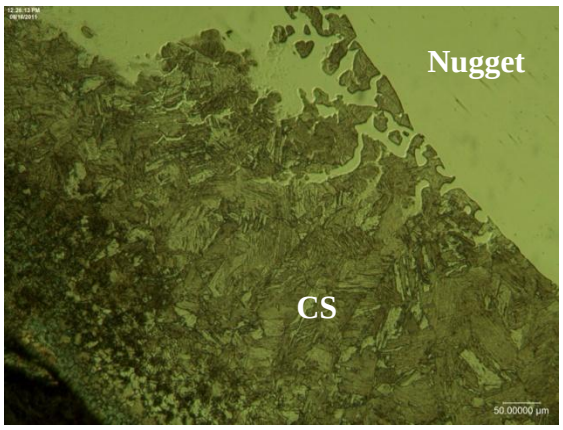

Fig. 12: HAZ microstructure of LCS side appearing the separated islands. (I = 3KA, t = 8 cycles).

At LCS side, the HAZ is gradually changing from martensitic structure adjacent to the fusion line to ferritic structure at the end of the HAZ with gradual decrease in grain size in the direction of heat transferred as shown in figure 12. When weld time increases, the weld nugget will far exceed melting temperature and internal pressure may expel molten metal from nugget to adjacent HAZ with minute metal particles giving the shape of separated islands in some places at fusion line as shown in figure 12.

Nugget structure showed in all joints a martensitic structure, which is the dominant structure in nugget zone. This is attributed to the high cooling rate of this welding process. Carbides were also observed near to the fusion line of the FSS side as shown in figure 13. Dilution from FSS enhances the formation of carbides. A layer also has been formed along fusion line and analyzed using EDX. Resulted element distribution curves are shown in figure 13. Chromium content decreases in the nugget direction.

The mode of failure was button pullout [10, 15] as shown in figure 14. Investigating the fractured specimens after tensile shear test, it was noticed that the crack has been initiated from the nugget tip then propagated towards the FSS side [10] as shown in figure 15. Crack propagation was intergranular through the FSS grains as shown in figure 16. Micro cracks were observed at the grain boundary of large ferritic grains where toughness and ductility reduced [16] as shown in figure 17. Micro voids were formed at the interface between the nugget and the formed layer in FSS side as shown in figure 15.

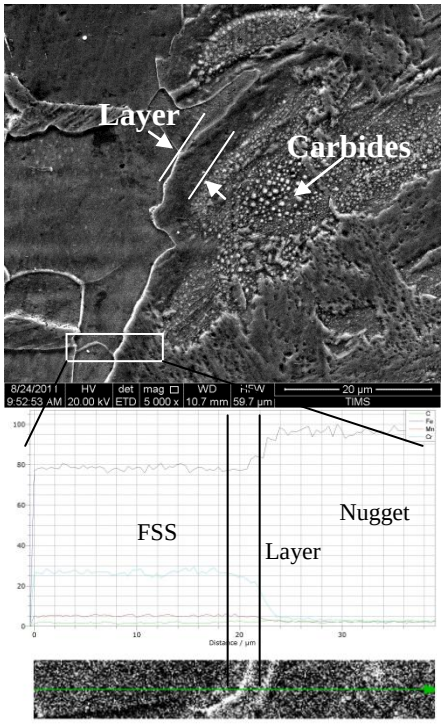

Fig. 13: Carbides formed and EDX distribution of alloying elements along formed layer at fusion line. Welding conditions: I = 3KA, t = 8cycles.

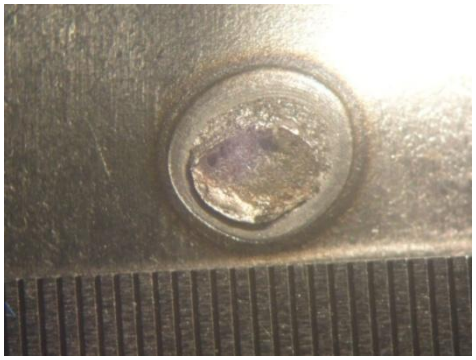

Fig. 14: Failure mode of spot dissimilar welded joint.

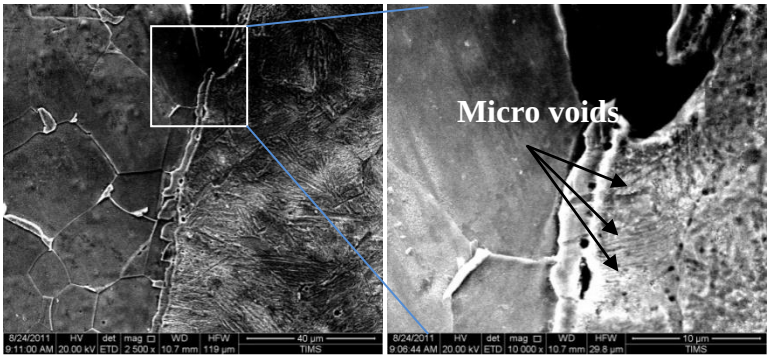

Fig. 15: Crack initiation after tensile shear test. I=3KA, t = 8cycles.

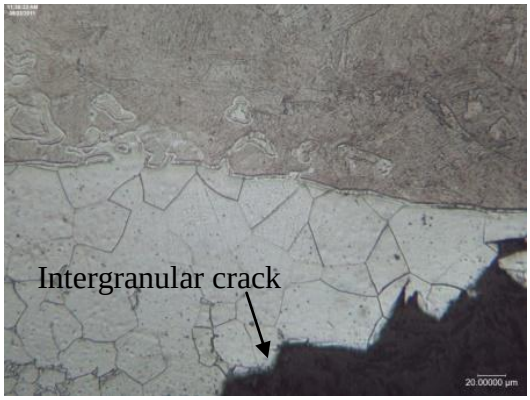

Fig. 16: Intergranular crack.

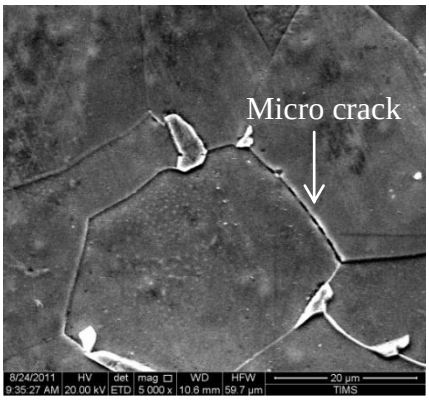

Fig. 17: Micro cracks formed at grain boundary of large ferritic grains.

3.5 Micro hardness

Micro hardness measurements were carried out alongside the nugget, starting from one tip and ending at the other. Two parallel lines of measurements were taken as schematically shown in figure 18(a). Figure 18(b) shows two nearly similar profiles. The higher values are resulted of formed martensite in nugget zone. [7, 9] In the FSS side, the micro hardness profile showed a little two peaks at the locations where the microstructure showed carbide formation.

Distribution of micro-hardness across thickness of joint is shown in figure 18(c). These are in a good agreement of results with the last findings where the highest value of micro hardness was recorded at the same places where the carbide formed shown in figure 13.

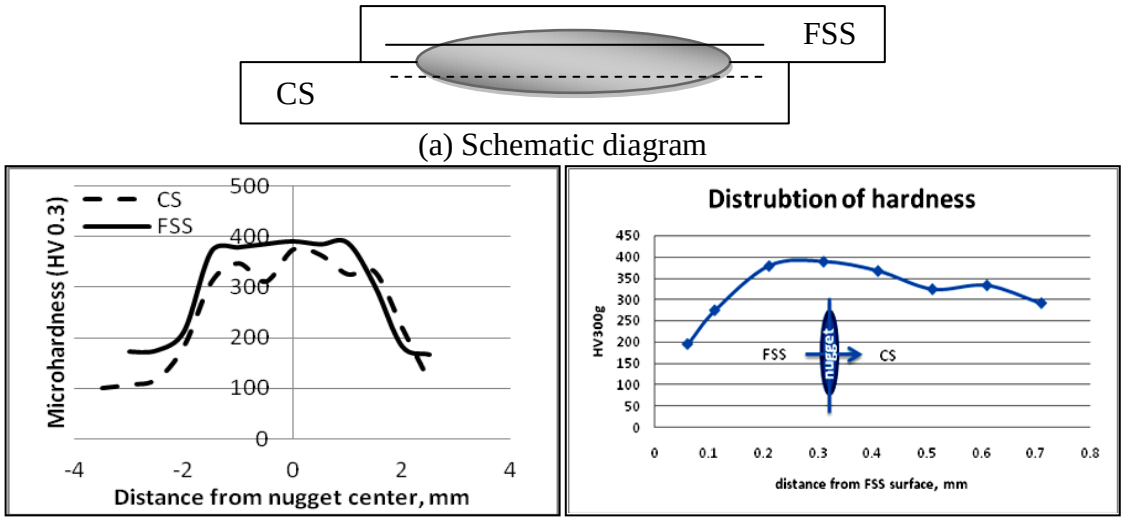

(a) Schematic diagram

(b) Micro hardness across nugget welded zones (c) Micro hardness through thickness.

Fig. 18: Micro hardness distribution for spot-welded joint at different locations, (I=3KA, t = 8cycles).

4. CONCLUSIONS

This work investigated the influence of main spot welding variables, welding current, welding time and electrode pressure, on the characteristic of dissimilar joint between LCS and FSS sheets. From the results obtained, it can be concluded that:

- The best electrode pressure in this combination of steels was 0.2MPa.
- Welding current is effective variable on weld quality.
- Rising current and time of welding enhance the weld strength up to certain values after which the spot welded joint strength reduces.
- The microstructure of the nugget is martensitic structure where joint cooling rate is high in the resistance spot welding operation.
- Crack initiated in tensile shear test at nugget tip and propagated in HAZ intergranularly of ferritic stainless steel side. Fracture mode was observed as button pullout.
- Micro hardness values had highest value where location of carbides existed adjacent to the fusion line.

5. REFERENCES

[1] Welding processes. AWS welding handbook, 7th ed., vol. 3, London, England, American Welding Society, Macmillan Press Ltd, (1980).

[2] Jadhav1, S.A. and Dr. Venkatesh, M. A.: "A review paper on optimization of process parameter of spot welding by multi-objective Taguchi", International Research Journal of Engineering and Technology (IRJET), vol. 03, Issue 05,pp. 2294-2297, (2016).

[3] Panday, A. K.; Khan, M. I. and Moeed, K. M.: "Optimization of resistance spot welding parameter by using Taguchimethod", International Journal of Engineering and Technology, vol.5, No. 02, pp. 234-239, (2013).

[4] Agashe, S. and Zhang, H.:"Selection of schedules based on heat balance in resistance spot welding". Welding J., 179S–83S. (2003).

[5] Kaluc, E.:"An effect of resistance spot welding parameters on the tensile shear strength and intergranular corrosion in the ferritic–austenitic stainless steels weldment". Ph. D. thesis, Istanbul Technical University, Institute of Applied Science, October, (1988).

[6] Norrish, J.:"Advanced welding processes". Bristol, Philadelphia and New York, United Kingdom: Institute of Physic Publishing, (1992).

[7] Vural, M. and Akkus, A.:"On the resistance spot weldability of galvanized interstitial free steel sheets with austenitic stainless steel sheets". J. Mater. Process Technol., 153–6, (2004).

[8] Bayram Kocabekir et. al.:"An effect of heat input, weld atmosphere and weld cooling conditions on the resistance spot weldability of 316L austenitic stainless steel", J. Mater. Proc. Tech., 195, pp. 327-335, (2008).

[9] Haanbaşoğlu, A. and Kaçar, R.: "Resistance spot weldability of dissimilar materials (AISI 316L-DIN 10130-99 steels)", J. Mater. & Design, 28, pp. 1794-1800, (2007).

[10] Marashi, P. et. al.:"Microstructure and failure behavior of dissimilar resistance spot-welds between low carbon galvanized and austenitic stainless steels", J. Mater. Sci. & Eng. A, 480, pp. 175-180, (2008).

[11] Sun, X.; Stephens, E. V.; Khaleel, M. A.; Shaw, H. and Kimchi, M.: "Resistance spot welding of Aluminum alloy to steel with transition material", from process to performance —Part I: Experimental Study, Welding Journal, 188-s to 195-s, (2004).

[12] Zhang, H. and Senkara, J.: "Resistance welding fundamentals and applications", CRC Press, pp. 61-67, (2006).

[13] Pouravari, M.; Mousavizadeh, S. M. and Marashi, S. P. H et. al.:"Influence of fusion zone size and failure mode on mechanical performance of dissimilar resistance spot welds of AISI 1008 low carbon steel and DP600 advanced high strength steel", J. Mater. & Design, 32, pp. 1390-1398, (2011).

[14] Pereira, A. M.; Ferreira, J. M. and Loureiro, A. et. al.:"Effect of process parameters on the strength of resistance spot welds in 6082-T6 aluminum alloy", J. Mater. & Design, 31, pp. 2454-2463, (2010).

[15] Hayat, F.:"The effects of the welding current on heat input, nugget geometry, and the mechanical and fractural properties of resistance spot welding on Mg/Al dissimilar materials", J. Mater.& Design, 32,pp. 2476-2484, (2011).

[16] Lippold, J. C. and Kotecki, D. J.:"Welding metallurgy and weldability of stainless steels", Wiley Interscience, pp. 114-115, (2005).

[17] Akkaş, N.: "Welding time effect on tensile-shear loading inresistance spot welding of SPA-H weathering steel sheets used in railway vehicles", ACTA PHYSICA POLONICA A,vol.131,pp. 52-54, (2017).
[18] Akkas, N. and Ilhan, E.: "Effect of welding current on mechanical properties of welding joints in SPAC steel sheets in resistance spot welding", ACTAPHYSICAPOLONICAA, vol.125,pp. 497-499,(2014).
[19]Pouranvari, M. and Marashi, S. P.: "Dissimilar spot welds of AISI 304/AISI 1008: Metallurgical and mechanical characterization", Steel Research Int. 82 No. 12, (2011).